

Table 5. Competitive Transport of Several M^{2+} vs. HT18C6 in an Emulsion Liquid Membrane

M^{2+}	Percent Transport		M^{2+}	Percent Transport	
	Cu^{2+} / M^{2+}			Cu^{2+} / M^{2+}	
Mn	99.6	/ 0.0	Sr	99.6	/ 3.8
Co	97.2	/ 6.7	Cd	97.2	/ 3.4
Ni	91.4	/ 0.0	Pb	92.4	/ 8.2
Zn	92.4	/ 8.2			

Transport after 7 minutes.

Table 6. Competitive Transport of Three Component Mixture in an Emulsion Liquid Membrane

M_1^{2+}	M_2^{2+}	Percent Transport		
		Cu^{2+}	M_1^{2+}	M_2^{2+}
Mn	/ Ni	87.0	/ 1.3	/ 2.2
Co	/ Cd	75.2	/ 0	/ 1.0
Zn	/ Sr	85.6	/ 0	/ 0
Cd	/ Pb	86.0	/ 1.6	/ 1.5

Transport after 7 minutes.

6 as carrier in this study. Significant transport was observed for Cu^{2+} over all the other metal ions tested. Experiments were carried out by placing equimolar amounts of Cu^{2+} ion and transition metal ions in the source phase. In Table 6 are listed experimental data of competitive transport for three component systems containing Cu^{2+} ion and two other metal ions. Binary result can in most case be extended to the ternary system since competition for a single ligand occur in both binary and ternary systems. Cu^{2+} was found the highest transport in each mixture. Log K data indicate that the Cu^{2+} -HT18C6 complex is more stable than those of transition metal cation, which is consistent with high Cu^{2+}

transport and low other metal ion transport in the HT18C6. Cu^{2+} bind the carrier in the membrane and is transported, while little carrier remains available to bind and transport other cations. The selective transport of Cu^{2+} over other cations with HT18C6 is a reflection of the greater affinity of HT18C6 for Cu^{2+} compared to that for the other cation. The highest degree of transport selectivity for Cu^{2+} by HT18C6 carrier in this emulsion membrane system employed may be applicable to remove Cu^{2+} from the solution containing several heavy metal ions, especially from waste water.

In a sense for commercial or analytical application, the emulsion membrane system can be employed for the separation of Cu^{2+} from several metal-containing species.

Acknowledgement. We gratefully acknowledge the financial support of the Korea Science Engineering Foundation and the basic science research institute program, Ministry of Education (1990) for this project.

References

1. J. P. Behr and J. M. Lehn, *J. Am. Chem. Soc.*, **107**, 241 (1985).
2. H. K. Lonsdale, *J. Membr. Sci.*, **10**, 81 (1982).
3. J. D. Way, R. D. Noble, T. M. Flynn, and E. D. Sloan, *J. Membr. Sci.*, **12**, 239 (1982).
4. M. H. Cho, K. H. Seon-Woo, and S. J. Kim, *Bull. Korean Chem. Soc.*, **9**, 5 (1988).
5. F. Nakashio and K. Kondo, *Sep. Sci. and Tech.*, **5**, 1171 (1980).
6. R. W. Baker, M. E. Tuttle, D. J. Kelly, and H. K. Lonsdale, *J. Membr. Sci.*, **2**, 213 (1977).
7. N. N. Li, *Ind. Eng. Chem., Process Des. Dev.*, **10**, 215 (1971).
8. R. M. Izatt, G. A. Clark, and J. J. Christensen, *J. Membr. Sci.*, **24**, 1 (1981).
9. R. M. Izatt and M. H. Cho, *J. Membr. Sci.*, **33**, 169 (1987).
10. R. M. Izatt, M. H. Cho, J. D. Lamb, and J. J. Christensen, *Anal. Chem.*, **59**, 19 (1987).

A Sensitivity Analysis for Three-Parameter Ellipsometry

Gyusung Chung, Duckhwan Lee*, and Woon-Kie Paik

Department of Chemistry, Sogang University, Seoul 121-742. Received April 25, 1991

In the three-parameter ellipsometry (TPE), also known as reflectance-ellipsometry, the ellipsometric measurements, Ψ and Δ , are combined with the reflectometric measurement, R , to determine the optical parameters and the thickness of a light-absorbing thin film. The constant Ψ , Δ , and R surfaces are analyzed graphically to understand the nature of the TPE solutions. A sensitivity analysis is shown to be useful not only for identifying the film properties which affect most the TPE measurements, but also for estimating errors in film properties arising from the uncertainties in measurements.

Introduction

In conventional ellipsometry, the change in the polarization

of the light reflected from surface covered by thin film is measured to determine the optical properties of the film^{1,2}. Because of the surface selectivity and the high sensitivity

of the ellipsometric measurements to the change of film properties, the ellipsometry has been a useful tool for studying thin films formed on substrates. For example, the passivation of metal surface has been extensively studied by this technique. Since *in situ* ellipsometry measurements can be performed in a short time, transient phenomena such as growth of film can also be studied by ellipsometry^{1,3}.

In ellipsometry using the three-phase model of an ambient medium-film-substrate system¹, the complex refractive index, $n_2 = n_2 - ik_2$, and the thickness, τ_2 , of the film are to be determined. However, two ellipsometric measurements, Ψ and Δ , are not in general sufficient to determine three unknown properties of the film, (n_2, k_2, τ_2) . In order to overcome this difficulty of the conventional ellipsometry, the reflectometric measurement is employed as the third supplementary measurement in the three-parameter ellipsometry (TPE)⁴. For this reason, the TPE has also been known as the reflectance-ellipsometry. The TPE is attractive from experimental point of view, since the reflectance R can be measured from the identical instrumental setup used for measuring Ψ and Δ with minimum modifications of the measurement routines. The TPE of this type has been successfully applied for studying thin surface films since early 1970's^{3,5-7}.

Even with the ideal three-phase model, the relations between the reflectance-ellipsometric measurements and the film properties are often cumbersome and require a numerical technique, such as the Newton-Rapson method⁸, to find the film properties corresponding to the experimental measurements. Furthermore, there are sometimes more than one set of solutions for a given set of experimental measurements⁹. There are even cases reported in which the TPE fails to give a solution^{1,9}. In this paper, the nature of the TPE solution is analyzed with three dimensional computer graphics and the contour diagrams. Despite the qualitative nature of the analysis, this type of study should provide more insight into the nature of solutions obtained in the TPE.

This paper also deals with the sensitivity analysis for the TPE. Mathematical modeling is often necessary to understand the nature of experimentally observed phenomena and/or to predict the experimental result. In mathematical modeling, many parameters are employed to represent experimental conditions and some fundamental characteristics of the system under investigation. Fundamental physical principles and some approximations if necessary are introduced to relate the parameters to the experimental measurements. In the TPE, for example, the three-phase model with the Fresnel equations is used to relate the experimental measurements to the properties of the film.

The difficulties in mathematical modeling arise from the uncertainties of the parameters in the model and the complicated relations between the parameters and the experimental measurements. Since the parameters in the model are seldom known to high precision, the predictions of the model are usually subject to uncertainty to some extent. More importantly, the complicated mathematical relations often makes it difficult to identify the parameter to which the experimental observations are sensitive. The sensitivity analysis addresses the question of quantitative role of parameters in the model predictions. It is also useful in estimating the parameter values fitting experimental data. The sensitivity analysis is an active research area in many different fields

such as chemistry, biology, and ecology. Applications of the sensitivity analysis in chemistry have been reviewed by Rabitz¹⁰.

In the TPE, there are three reflectometric and ellipsometric measurements, (Ψ, Δ, R) . And, the optical constants and the thickness, (n_2, k_2, τ_2) , of the film are the parameters to be determined in the three-phase model. The refractive index of the transparent ambient medium n_1 , and the optical constant of the substrate, $n_3 = n_3 - ik_3$, as well as the wavelength, λ , and the angle of incidence of the light, ϕ_1 , are also included in the parameters. In this case, the measurements and the parameters are related by the Fresnel equations¹. Because of the complexities of the relations in the TPE, it is not evident at all how the measurements are affected by changes in the parameters. The question of sensitivity is thus important to understand the nature of the ellipsometric-reflectometric measurements and to select the optimum experimental conditions for the TPE. For example, the ellipsometric measurements have been known as strongly dependent upon the angle of incidence of the light. Thus, the choice of incident angle is an important factor for the success of the TPE. The sensitivity analysis can provide the criteria for choosing the best possible angle of incidence.

In this paper, we present the forward sensitivity analysis (FSA), in which the sensitivities of the ellipsometric-reflectometric measurements with respect to the film properties are analyzed by using the analytical expressions for the partial derivatives. We also present the reverse sensitivity analysis (RSA), in which the sensitivities of the film properties with respect to the experimental measurements are studied. The FSA is helpful in understanding the characteristics of the TPE measurements, while the RSA provides the information on choosing the optimum experimental conditions. The dependence of the ellipsometric and reflectometric measurements on the film thickness was studied by Azzam and Bashara¹.

Three-Parameter Ellipsometry

In this Section, a brief theoretical basis for the three-parameter ellipsometry is described in order to define the notations used in this paper. The details of the theory can be found elsewhere^{1,2,4,11}.

The ellipsometric and reflectometric measurements, (Ψ, Δ, R) , are defined as following,

$$\tan \Psi e^{i\Delta} = \frac{r_p}{r_s} \quad (1)$$

$$R = (100/2) (|r_p|^2 + |r_s|^2) \quad (2)$$

where r_p and r_s are the overall complex reflection coefficients for polarizations that are parallel and perpendicular to the plane of incidence, respectively. The constant factor of 100 in Eq. (2) is for the conversion of the fractional reflectance to percentage. All of these three measurements, Ψ , Δ , and R , can be obtained simultaneously from a single experimental setup, thus making the TPE attractive from experimental point of view.

The three-phase model as shown in Figure 1, in which the film is regarded as optically homogeneous, is often employed to interpret the TPE result. With this model, the

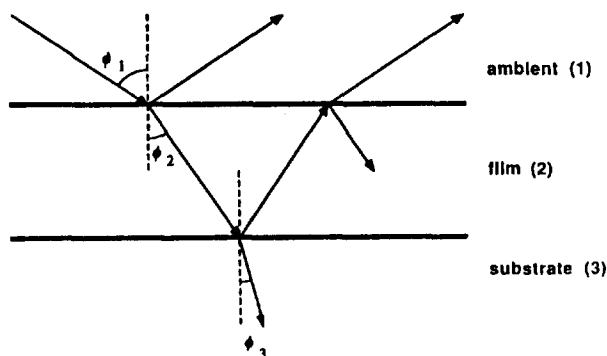


Figure 1. Three-phase model for ellipsometry.

complex reflection coefficients, r_p and r_s , can be expressed, according to the Fresnel equations, as

$$r_p = \frac{r_{12p} + r_{23p} \exp(-iD)}{1 + r_{12p} r_{23p} \exp(-iD)} \quad (3a)$$

$$r_s = \frac{r_{12s} + r_{23s} \exp(-iD)}{1 + r_{12s} r_{23s} \exp(-iD)} \quad (3b)$$

The ambient medium, the film, and the substrate are denoted by 1, 2, and 3, respectively, in the subscripts of the r 's. $D = (4\pi/\lambda) \tau_2 n_2 \cos \phi_2$ is the change of phase angle inside the film. And, r_{ijp} and r_{ijs} are the Fresnel reflection coefficients at the interface between the i -th and j -th phase,

$$r_{ijp} = \frac{n_j \cos \phi_i - n_i \cos \phi_j}{n_j \cos \phi_i + n_i \cos \phi_j} \quad (4a)$$

$$r_{ijs} = \frac{n_i \cos \phi_i - n_j \cos \phi_j}{n_i \cos \phi_i + n_j \cos \phi_j} \quad (4b)$$

The p and s in the subscripts of the r 's represent the polarizations parallel and perpendicular to the plane of incidence, respectively, and $n_i = n_i - ik_i$ is the complex refractive index of the i -th phase. The incident angles, $\{\phi_i\}$, in the individual media are related by the Snell's law,

$$n_1 \sin \phi_1 = n_2 \sin \phi_2 = n_3 \sin \phi_3 \quad (5)$$

With the three-phase model, the experimental measurements in the TPE depend not only upon the properties of the film but also upon the optical properties of the ambient medium and the substrate as well as the properties of the incident light. A judicious choice of the ambient medium and the incident angle of the light is required to get reasonable measurements. In order to find the optical properties and the thickness of the film corresponding to the experimental measurements, one should invert Eqs. (1) and (2) for (n_2, k_2, τ_2) in terms of (Ψ, Δ, R) . Since these equations cannot be inverted analytically, however, a numerical iteration procedure such as the Newton-Rapson technique⁸ should be adopted^{3,9}. In this procedure, a set of trial values for the film properties are successively modified until the experimentally measured values of (Ψ, Δ, R) are obtained. It is possible to write an efficient computer program for this purpose using the following analytical expressions for the partial derivatives.

$$\left(\frac{\partial \Psi}{\partial \alpha}\right)_{\beta, \gamma} = 0.5 \sin 2\Psi \operatorname{Re} \left[\frac{1}{r_p} \left(\frac{\partial r_p}{\partial \alpha}\right)_{\beta, \gamma} - \frac{1}{r_s} \left(\frac{\partial r_s}{\partial \alpha}\right)_{\beta, \gamma} \right] \quad (7a)$$

$$\left(\frac{\partial \Delta}{\partial \alpha}\right)_{\beta, \gamma} = \operatorname{Im} \left[\frac{1}{r_p} \left(\frac{\partial r_p}{\partial \alpha}\right)_{\beta, \gamma} - \frac{1}{r_s} \left(\frac{\partial r_s}{\partial \alpha}\right)_{\beta, \gamma} \right] \quad (7b)$$

$$\left(\frac{\partial R}{\partial \alpha}\right)_{\beta, \gamma} = 100 \operatorname{Re} \left[r_p^* \left(\frac{\partial r_p}{\partial \alpha}\right)_{\beta, \gamma} + r_s^* \left(\frac{\partial r_s}{\partial \alpha}\right)_{\beta, \gamma} \right] \quad (7c)$$

Here, α , β , and γ represent the film properties, n_2 , k_2 , or τ_2 . $\operatorname{Re}[z]$ and $\operatorname{Im}[z]$ are the real and the imaginary parts of a complex z , respectively. The complex conjugate of z is denoted as z^* in Eq. (7c). The analytical partial derivatives of the overall complex reflection coefficients with respect to the film properties can be readily derived from Eq. (3)⁹.

With the Newton-Rapson technique, a few trials of the initial guess of the film properties are usually sufficient to find the solutions corresponding to the experimental measurements. There are sometimes two sets of the film properties, for a given set to experimental measurements, found from different initial trial values for the film properties¹. They are often called "metal" and "water" branch solutions⁹ when aqueous solution is used as ambient medium. Only one set of the solutions are accepted as physically meaningful.

In order to study the nature of the TPE solutions, the surfaces of constant Ψ , Δ , and R are analyzed qualitatively by using the three-dimensional graphics and contour diagrams. Assuming certain values of the optical properties of the film, n_2 and k_2 , the thickness of the film, τ_2 , can be found numerically from Eqs. (1) and (2), which give the experimental value of Ψ , Δ , or R . Repeating this process within reasonable ranges of n_2 and k_2 , one can construct, in the n_2 - k_2 - τ_2 space, the surfaces of constant Ψ , Δ , and R . The ellipsometric solutions are given as the points at which all these three surfaces intersect. The intersecting points can be more closely examined by using the contour maps of these surfaces.

The construction of the surfaces of constant Ψ , Δ , and R becomes complicated for thick films because of the quasi-periodic natures of Ψ , Δ , and R with respect to τ_2 due to the presence of $\exp(-iD)$ in Eq. (3). However, passive films formed on metal surfaces as thick as several hundred angstroms can be studied without such difficulty.

Forward and Reverse Sensitivities

A need for sensitivity analysis for the TPE can be recognized by the complexities of Eqs. (1) and (2) relating the ellipsometric-reflectometric measurements to the film properties. From these relations, it is not evident at all which properties of the film control the experimental measurements and how the uncertainties in the experimental measurements affect the properties of the film to be determined. This kind of information are important to understand the nature of the TPE as well as to estimate the accuracy of the film properties determined by the TPE. It is also important to find out the optimum experimental conditions for the TPE.

The forward sensitivity coefficients (FSC's) are defined by Eq. (7). They represent how the ellipsometric-reflectometric measurements are affected by the changes of the optical constants and the thickness of the film. For example, $(\partial \Psi / \partial n_2)_{k_2, \tau_2}$ is the rate of change of Ψ with respect to n_2 when k_2 and τ_2 of the film are kept constant. Thus, by analyzing the nine such FSC's, one can identify quantitatively which properties of the film, n_2 , k_2 , and/or τ_2 , control the

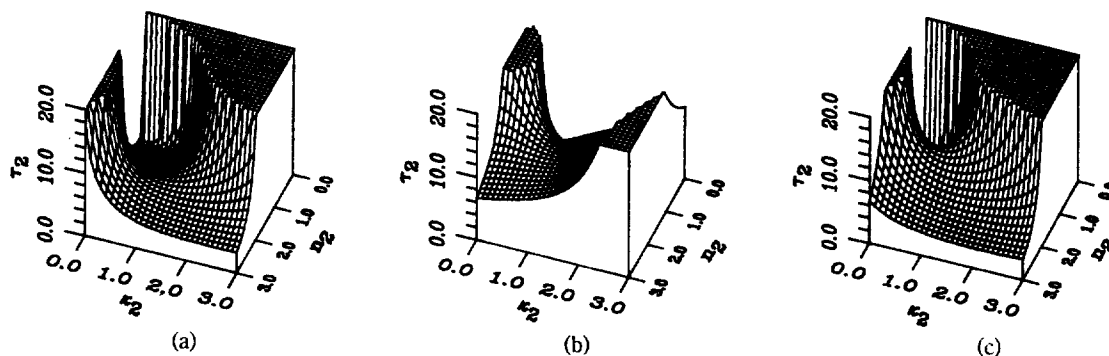


Figure 2. The surfaces of constant (a) Ψ , (b) Δ , and (c) R for passive film formed on Ni surface. The experimental data are taken from Ref. 3. The angle of incidence is 55° and the wavelength is 632.8 nm.

magnitude of an ellipsometric or reflectometric measurement.

On the other hand, the reverse sensitivity coefficients (RSC's) are defined by the partial derivatives of the form of $(\partial\alpha_i/\partial M_j)_{M_k, M_l}$. Here, α_i is one of the film properties and M_j 's represent the experimental measurements, (Ψ , Δ , R). These RSC's indicate how sensitive the film properties are with respect to the experimental measurements. For example, $(\partial n_2/\partial \Psi)_{\Delta, R}$ is the rate of change of n_2 with respect to Ψ when the other experimental measurements, Δ and R , are kept constant. Thus, these RSC's can be regarded as representing the extents of error in the film properties determined by the TPE arising from experimental inaccuracies in measurements.

Since Eqs. (1) and (2) cannot be analytically inverted for n_2 , k_2 , and τ_2 , it is not possible to find directly the expressions for the RSC's. However, the partial derivatives used for the FSC's in Eq. (7) can be utilized and the RSC's can be written in the following form¹².

$$\left(\frac{\partial \alpha_i}{\partial M_j}\right)_{M_k, M_l} = -\frac{J^{ji}}{g} \quad (8)$$

Here, α_i denotes n_2 , k_2 , and τ_2 for $i=1, 2$, and 3, respectively. M_j 's represent the ellipsometric-reflectometric measurements, Ψ , Δ , or R . And, g is the Jacobian determinant¹² given as

$$g = \begin{vmatrix} \left(\frac{\partial \Psi}{\partial n_2}\right)_{k_2, \tau_2} & \left(\frac{\partial \Psi}{\partial k_2}\right)_{n_2, \tau_2} & \left(\frac{\partial \Psi}{\partial \tau_2}\right)_{n_2, k_2} \\ \left(\frac{\partial \Delta}{\partial n_2}\right)_{k_2, \tau_2} & \left(\frac{\partial \Delta}{\partial k_2}\right)_{n_2, \tau_2} & \left(\frac{\partial \Delta}{\partial \tau_2}\right)_{n_2, k_2} \\ \left(\frac{\partial R}{\partial n_2}\right)_{k_2, \tau_2} & \left(\frac{\partial R}{\partial k_2}\right)_{n_2, \tau_2} & \left(\frac{\partial R}{\partial \tau_2}\right)_{n_2, k_2} \end{vmatrix} \quad (9)$$

J^{ji} in Eq. (8) is the cofactor of the Jacobian determinant for the (j, i) element, which is $(-1)^{i+j}$ times the complementary minor of the (j, i) element of g .

Results and Discussion

In this Section, we present the results obtained for nickel oxide film formed on nickel surface in the process of electrochemical passivation in weakly acidic solution³. For our analysis, we have chosen the case in which $\delta\Psi = -0.128^\circ$, $\delta\Delta = -1.077$ and $\delta R = -0.854$ at $\phi_1 = 55^\circ$ with $\lambda = 632.8$ nm.

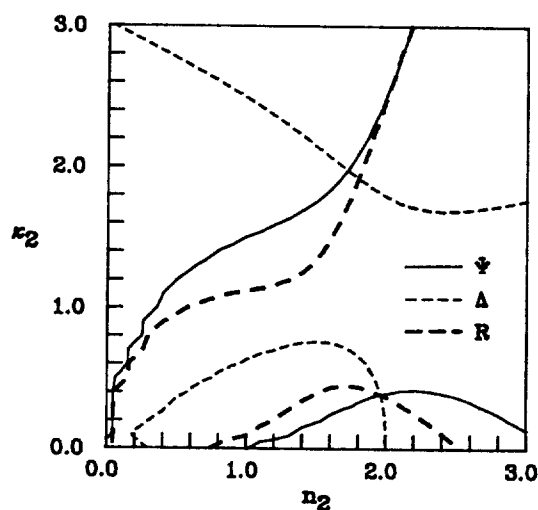


Figure 3. Contour map of the Ψ , Δ and R surfaces for passive film on Ni. All contour lines correspond to $\tau_2 = 11.6 \text{ \AA}$.

The film properties for this case are determined as $n_2 = 1.96$, $k_2 = 0.38$, and $\tau_2 = 11.6 \text{ \AA}$. We also found the other set of solutions, $n_2 = 1.86$, $k_2 = 2.54$, and $\tau_2 = 17.9 \text{ \AA}$, where k_2 is clearly too large to be acceptable. Thus, the former set of the solutions has been accepted as physically meaningful. The results presented in this section are selected from much larger set of calculations and they are believed to exhibit the typical characteristic features of the TPE.

Constant Ψ , Δ , and R Surfaces. In Figure 2, the constant Ψ , Δ , and R surfaces are presented. A point on the Ψ surface, for example, represents the hypothetical film with (n_2, k_2, τ_2) which would give rise to the experimental value of Ψ irrespective of the values of Δ and R . The constant Δ and R surfaces can be interpreted similarly. The surfaces are cut at $\tau_2 = 20.0 \text{ \AA}$ for the sake of convenience and the flat parts on the top of the surfaces are the artifact. The optical properties of the real film, which is the solution for the TPE, is given as the point at which these three surfaces intersect simultaneously. The intersecting point can be more closely examined from the contour map in Figure 3. The contour lines for Ψ , Δ , and R in the upper region of Figure 3 intersect at $\tau_2 = 17.9 \text{ \AA}$ which corresponds to the second set of the solutions mentioned above.

As shown in Figure 2, the constant Ψ , Δ and R surfaces are in general saddle-shaped with a valley in the middle

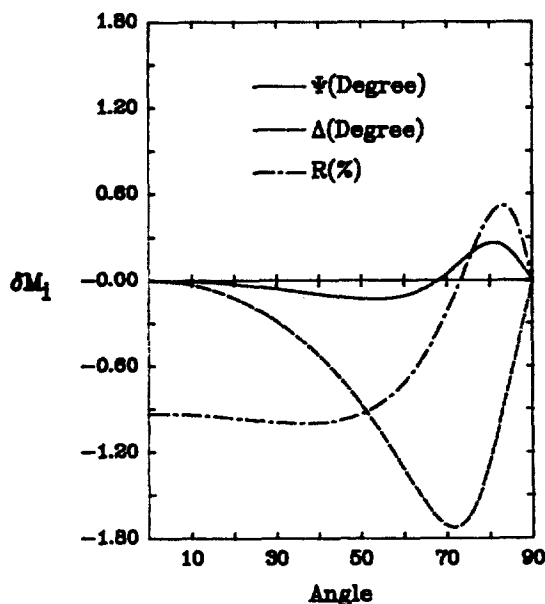


Figure 4. Changes in Ψ , Δ , and R produced by passive film formation as function of the angle of incidence, calculated for experimental conditions of Figure 2.

and steep walls at small and large k_2 . In many cases, the constant Δ surface appears to be relatively flat compared to the constant Ψ and R surfaces. The shapes of the constant Ψ and R surfaces change drastically with the experimental values, while the shape of Δ surface is relatively insensitive to the experimental value. Especially, the regions of steep wall in the Ψ and R surfaces change significantly for small changes of Ψ and R .

The three surfaces usually intersect simultaneously in the regions where the walls start to rise from the saddle region. The presence of the multiple solutions can be understood from Figure 2 and 3 as arising from the saddle shapes of these surfaces. Since the shape of the saddle point regions for the constant Ψ and R surfaces changes drastically with the experimental values, the TPE solutions are expected to be very sensitive to the measurements of Ψ and R . This can be seen more quantitatively in the sensitivity analysis presented below.

It is also noted that the walls of the constant Ψ and R surfaces are very similar. In Figure 3, it can be seen that the contour lines for Ψ and R run nearly parallel to each

other. If these two contour lines run parallel without crossing each other, then TPE should fail to give a solution. It was possible indeed to make two contour lines parallel, thus making the TPE fail, by simply changing the experimental values by small amounts which can be considered as experimental errors. We believe that the failure of the TPE reported earlier⁹ is due to errors in experimental measurements, especially in Ψ and/or R .

In addition, it is also noted that the shapes of the constant Ψ , Δ , and R surfaces depend significantly upon the experimental conditions, especially on the angle of incidence, because $\delta\Psi$, $\delta\Delta$, and δR vary with the angle of incidence as shown in Figure 4. Here, δM_i denotes the change of the optical measurement, M_i , produced by film formation. We found that as the angle of incidence increases, the walls of Figure 2 in general become fatter and the valley near the saddle point region goes up as shown in Figure 5. Furthermore, the contour lines of Ψ and R appear to become more parallel for large incidence angle, thus increasing the possibility of the failure of the TPE. Therefore, it seems that a choice of too large angle of incidence should be avoided for the success of the TPE. It can be seen again that the constant Δ surface is relatively insensitive to the change of experimental conditions compared to the constant Ψ and R surfaces. The change of surface shape with the angle of incidence can be utilized to resolve the difficulty in finding TPE solutions by employing a slightly different angle of incidence for TPE experiment. It is noted in this regard that the measurement of R is very sensitive to fluctuations in experimental setup.

Sensitivity Analysis. There are nine FSC's and nine RSC's as defined in Eq. (7) and (8), respectively. These coefficients vary with the experimental conditions such as the angle of incidence, the optical properties of the ambient medium and the substrate, the wavelength of the light. Among these factors, the angle of incidence is the most important one affecting the sensitivities. It is noted that only the magnitude of the sensitivity coefficients are important.

In order to compare the sensitivities for the three optical properties of the film, we normalize the sensitivity coefficients with the experimentally determined optical properties of the film, α_i^{exp} . In other words, $\alpha_i/\alpha_i^{\text{exp}}$ is used instead of the optical properties of the film α_i for the sensitivity coefficients in Eqs. (7) and (8). The normalized FSC, $(\partial M_i/\partial \alpha_i)_0$, now represents the sensitivity of the measurement M_i ($=\Psi$, Δ , or R) for the fractional change of the film property,

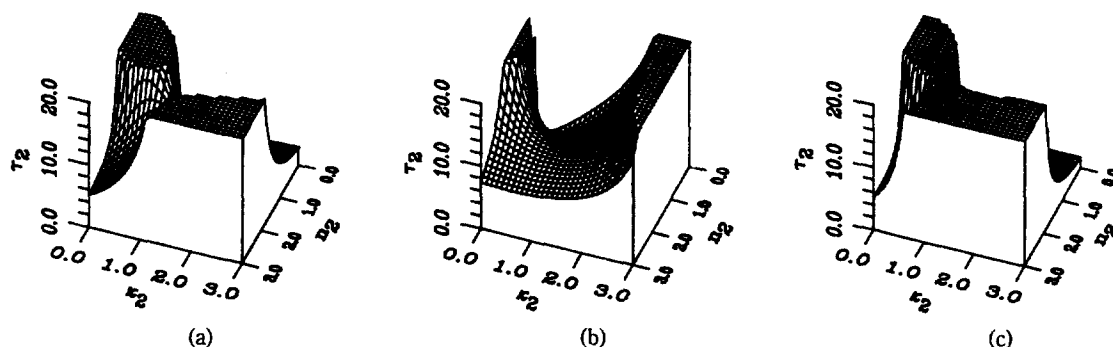


Figure 5. The surfaces of constant (a) Ψ , (b) Δ , and (c) R for passive film formed on Ni surface when the angle of incidence is 80° . The same passive film as in Figure 2 is assumed.

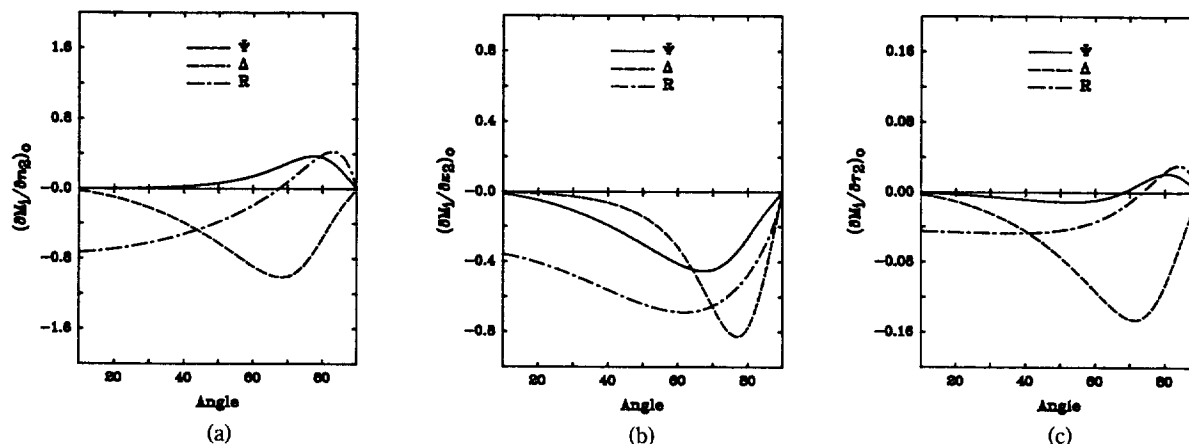


Figure 6. The dependencies, on the angle of incidence, of the normalized forward sensitivity coefficients with respect to (a) n_2 , (b) k_2 , and (c) τ_2 . The same passive film as in Figure 5 is assumed.

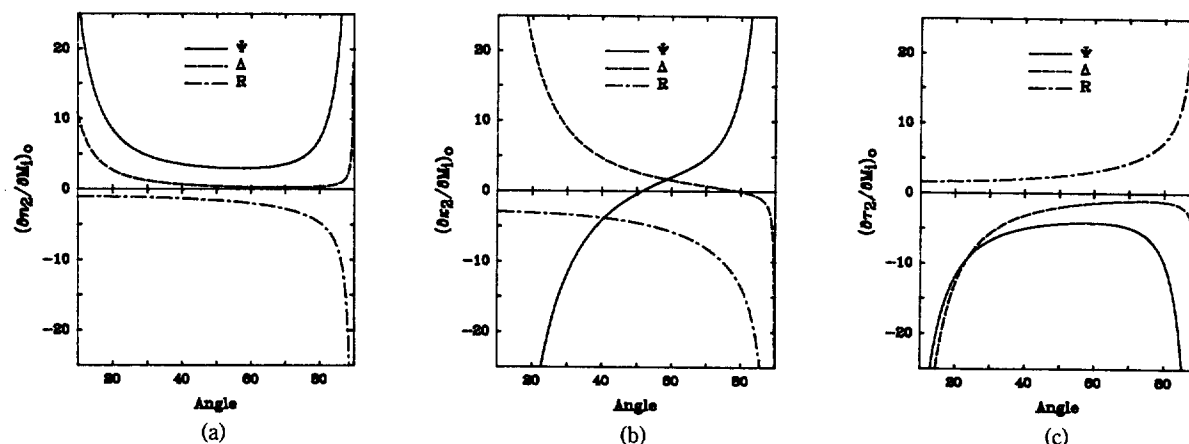


Figure 7. The dependencies, on the angle of incidence, of the normalized reverse sensitivity coefficients of (a) n_2 , (b) k_2 , and (c) τ_2 . The same passive film as in Figure 2 is assumed.

$\alpha_j/\alpha_j^{\text{exp}}$. Likewise, the normalized RSC, $(\partial\alpha_j/\partial M_i)_0$, is the fractional change of the film property, $\alpha_j/\alpha_j^{\text{exp}}$, caused by infinitesimal change in experimental measurement M_i .

Figures 6 and 7 show the dependencies of the normalized FSC's and RSC's, respectively, on the angle of incidence, ϕ_1 , for the case of passive film formed on Ni surface. These are the typical cases for passive films on metal surfaces which we studied most extensively using the TPE. It is seen that the sensitivity coefficients are strongly dependent on ϕ_1 . For the air-gold-glass system studied by Azzam and Bashara¹ in which the substrate is transparent, the singularities at the Brewster angle are observed in the FSC's with respect to τ_2 . However, such singularities are absent for the passive films on light absorbing Ni surface. The sensitivity coefficient for the air-gold-glass systems show in general the features similar to those presented below.

From Figure 6, it is seen that, in the range of incident angle between 50° and 70° , Δ and R are more sensitive than Ψ to all of the film properties, n_2 , k_2 and τ_2 . On the other hand, Ψ is fairly sensitive to k_2 . When $\phi_1=55^\circ$, which is a judicious choice of incident angle in the TPE⁴, Δ is most sensitive to n_2 and τ_2 , while R is most sensitive to k_2 . Furthermore, Ψ is least sensitive to n_2 and τ_2 . In the case of air-gold-glass system¹, R is almost independent of

k_2 and τ_2 while Ψ and Δ are sensitive to the film properties when ϕ_1 is close to the Brewster angle. Especially in air-gold-glass case, Δ is most sensitive to the film properties.

This type of information is important in understanding the characteristics of ellipsometric-reflectometric measurements. For example, when the film with the constant complex refractive index is growing on a substrate, Δ is the most sensitively changing ellipsometric measurement and Ψ remains almost constant. This is indeed the case which is seen from the growth of passive film on Ni surface^{3,7}. Furthermore, this type of information can provide important criteria for determining optimum angle of incidence for the TPE experiment. It is seen from Figure 6 that the TPE measurements might appear most sensitive to the change of film properties when ϕ_1 is between 70° and 80° . It is interesting to note that $\phi_1 \approx 70^\circ$ has been widely used in the conventional two-parameter ellipsometry. It has been however pointed out later^{4,11} that the change of the TPE measurements with the angle of incidence, as shown in Figure 4, should also be taken into account for determining the optimum angle of incidence.

The RSC's are the convenient measures of the relative errors of the film properties determined from the experimental TPE measurement which are inevitably subject to some

extent of experimental uncertainties. Figure 7 shows typical dependencies, on the angle of incidence, of normalized RSC's of the same system as for the Figure 6. According to Figure 7, n_2 is least sensitive to Δ and most sensitive to Ψ for wide range of ϕ_1 . At $\phi_1=55^\circ$, k_2 and τ_2 are most sensitive to R and Ψ , respectively, while τ_2 is least sensitive to Δ . Thus, for example, the experimental error in Δ would not affect the values of n_2 and τ_2 as much as the errors in Ψ and R . This agrees with the observations made earlier based on the shapes of the constant Ψ , Δ , and R surfaces. If the thickness of the film, τ_2 , is the most important property to be determined, then Ψ and R should be carefully measured.

From these RSC's, it can be clearly seen that the properties of the film are very sensitive to Ψ and R at $\phi_1 \approx 70^\circ$. At this angle of incidence, any experimental errors in Ψ , and R would be magnified in n_2 , k_2 , and τ_2 , thus making experiment extremely difficult. Moreover, it is also noted that the measurement of R is most susceptible to fluctuations in the experimental set-up. This agrees with the previous conclusion of Paik *et al.*⁴ in which $\phi_1 \approx 55^\circ$ is preferred over $\phi_1 \approx 70^\circ$ used in the conventional two-parameter ellipsometry.

The sensitivity coefficients are also affected by the refractive index of the ambient medium, n_1 . As n_1 increases, the RSC's generally increase slightly in magnitudes although the overall dependencies on ϕ_1 are similar to Figure 7. The optical properties of the substrate also show minor effect on the RSC's.

In order to determine the optimum experimental conditions, the measurements should be sensitive enough to discern the films of different physical properties. At the same time, the film properties to be determined should not be too sensitive to the experimental errors in the measurements. Therefore, both of the FSC's and RSC's should be carefully examined to find the optimum compromise.

In this paper, we clarified the nature of the solutions for the film properties obtained by the TPE by closely examining the constant Ψ , Δ , and R surfaces. We also identified,

through the FSA, the properties of the film which affect most the ellipsometric-reflectometric measurements. Furthermore, it is shown that the RSA can provide a measure of estimating errors in film properties arising from the experimental uncertainties in measurements. It is also shown that the optimum experimental conditions can be determined by sensitivity analysis.

Acknowledgment. This work was supported by the Korean Science and Engineering Foundation and the Ministry of Education of Korea. One of us (GC) is grateful for the Graduate Research Fellowship of the Korean Science and Engineering Foundation.

References

1. R. M. A. Azzam and N. M. Bashara, in: *Ellipsometry and Polarized Light* (North-Holland, Amsterdam, 1987).
2. S. Gottesfeld, in: *Electroanalytical Chemistry*, **15**, 143, ed., A. J. Bard (Marcel Dekker, New York, 1989).
3. (a) Y. Kang and W. Paik, *Surf. Sci.*, **182**, 257 (1987); (b) Y. Kang, Thesis, (Sogang University, Seoul, 1985).
4. W. Paik and J. O'M. Bockris, *Surf. Sci.*, **28**, 61 (1971).
5. J. Horkans, B. C. Cahan, and E. Yeager, *Surf. Sci.*, **46**, 1 (1974).
6. S. Gottesfeld, M. Babai, and B. Reichman, *Surf. Sci.*, **56**, 373 (1976).
7. W. Paik and Z. Szklarska-Smilalowska, *Surf. Sci.*, **96**, 401 (1980).
8. S. S. Kuo, in: *Computer Applications of Numerical Method* (Addison-Wesley, New York, 1971).
9. B. D. Cahan, *Surf. Sci.*, **56**, 354 (1976).
10. H. Rabitz, M. Kramer, and D. Dacol, *Ann. Rev. Phys. Chem.*, **34**, 419 (1983).
11. W. Paik, in: *International Review of Science, Physical Chemistry Series One*, Vol. **6**, J. O'M Bockris, ed., (Butterworth, London, 1973).
12. F. B. Hilderbrand, in: *Advanced Calculus for Applications*, 2nd ed. (Prentice-Hall, Englewood Cliff, 1976).

Synthesis of New Tetraaza Macrocylic Ligands with Cyclohexane Rings and their Ni(II) and Cu(II) Complexes

Shin-Geol Kang*, Jae Keun Kweon, and Soo-Kyung Jung

Department of Chemistry, Taegu University, Kyungsan 713-714. Received May 15, 1991

The tetraaza macrocylic ligand 3,14-dimethyl-2,6,13,17-tetraazatricyclo[14,4,0^{1,18},0^{7,12}]docosa-2,12-diene(B), that contains two cyclohexane rings, has been prepared as its dihydroperchlorate salt by the nontemplate condensation of methyl vinyl ketone with 1,2-diaminocyclohexane and perchloric acid. Reduction of B with sodium borohydride produces 3,14-dimethyl-2,6,13,17-tetraazatricyclo[14,4,0^{1,18},0^{7,12}]docosane(C). Square planar Ni(II) and Cu(II) complexes of B and C have been prepared by the reaction of the metal ions and the ligands. Synthesis, characterization, and the properties of the ligands and their metal complexes are reported.

Introduction

Synthetic polyaza macrocycles and their metal complexes

often exhibit unusual chemical properties which enable practical applications of these compounds.¹⁻¹³ Since the properties of the macrocylic compounds are correlated with struc-